Peptidoglycan-binding protein TsaP functions in surface assembly of type IV pili

Katja Siewering[a,1], Samta Jain[a,1,2], Carmen Friedrich[a], Mariam T. Webber-Birungi[b], Dmitry A. Semchonok[b], Ina Binzen[a], Alexander Wagner[a], Stuart Huntley[a], Jörg Kahnt[a], Andreas Klingl[c], Egbert J. Boekema[b], Lotte Søgaard-Andersen[a], and Chris van der Does[a,3]

[a]Department of Ecophysiology, Max Planck Institute for Terrestrial Microbiology, D-35043 Marburg, Germany; [b]Department of Electron Microscopy, Groningen Biomolecular Sciences and Biotechnology Institute, University of Groningen, Nijenborgh 7, 9747 AG, Groningen, The Netherlands; and [c]Cell Biology and Landes-Offensive zur Entwicklung Wissenschaftlich-ökonomischer Exzellenz Research Centre for Synthetic Microbiology, Philipps-Universität Marburg, D-35043 Marburg, Germany

Edited by Thomas J. Silhavy, Princeton University, Princeton, NJ, and approved January 21, 2014 (received for review December 9, 2013)

Type IV pili (T4P) are ubiquitous and versatile bacterial cell surface structures involved in adhesion to host cells, biofilm formation, motility, and DNA uptake. In Gram-negative bacteria, T4P pass the outer membrane (OM) through the large, oligomeric, ring-shaped secretin complex. In the β-proteobacterium *Neisseria gonorrhoeae*, the native PilQ secretin ring embedded in OM sheets is surrounded by an additional peripheral structure, consisting of a peripheral ring and seven extending spikes. To unravel proteins important for formation of this additional structure, we identified proteins that are present with PilQ in the OM. One such protein, which we name T4P secretin-associated protein (TsaP), was identified as a phylogenetically widely conserved component of the secretin complex that co-occurs with genes for T4P in Gram-negative bacteria. TsaP contains an N-terminal carbohydrate-binding lysin motif (LysM) domain and a C-terminal domain of unknown function. In *N. gonorrhoeae*, lack of TsaP results in the formation of membrane protrusions containing multiple T4P, concomitant with reduced formation of surface-exposed T4P. Lack of TsaP did not affect the oligomeric state of PilQ, but resulted in loss of the peripheral structure around the PilQ secretin. TsaP binds peptidoglycan and associates strongly with the OM in a PilQ-dependent manner. In the δ-proteobacterium *Myxococcus xanthus*, TsaP is also important for surface assembly of T4P, and it accumulates and localizes in a PilQ-dependent manner to the cell poles. Our results show that TsaP is a novel protein associated with T4P function and suggest that TsaP functions to anchor the secretin complex to the peptidoglycan.

Type IV pili systems (T4PSs) are involved in the assembly of long, thin fibers, which are found on the surfaces of many bacteria and archaea (1). Type IV pili (T4P) function in host cell adhesion, twitching motility, virulence, DNA uptake, and biofilm formation and are evolutionary related to type II secretion systems (T2SSs), bacterial transformation systems, and the archaellum (2–4). T4PSs can be divided into T4aPSs and T4bPSs that are distinguished based on pilin size and assembly systems (5, 6). T4aPSs form the most abundant class, and the T4P formed by these systems can undergo cycles of extension, adhesion, and retraction, which is a feature that distinguishes them from the other bacterial surface structures (7, 8). T4aP retract at rates up to 1 μm/s and can generate forces up to 150 pN (9, 10). Generally, T4bPSs are not associated with retraction. Here, we focus on T4aPSs and refer to these as T4PSs unless specifically indicated. T4PSs have been studied extensively in many bacteria but are especially well characterized in *Neisseria* and *Pseudomonas* spp. and in *Myxococcus xanthus*. Different nomenclature is used for different T4PSs (Table S1). Here, the *Neisseria gonorrhoeae* nomenclature is used.

T4P are composed of major (e.g., PilE) and minor (in *N. gonorrhoeae*; e.g., PilV, PilX, ComP) pilins that are synthesized as preproteins with a type III signal peptide. After cleavage of the signal peptide by the prepilin peptidase PilD (11, 12), the T4P are assembled by a multiprotein complex (13). In Gram-negative bacteria, the proteins of T4PSs can be divided into three subcomplexes: the inner membrane (IM) motor complex, the alignment complex, and the outer membrane (OM) pore complex (6). The IM motor complex drives both the assembly and the retraction of T4P. Pilin subunits are extruded from the IM by the platform protein PilG (14) and the hexameric ATPase PilF (15). Disassembly of T4P with retraction occurs when PilF is replaced by the hexameric ATPase PilT (7, 16). PilU, a PilT paralog, is involved in retraction to a lesser extent (17). The alignment complex consisting of PilM, PilN, PilO, and PilP is proposed to connect the IM motor complex and the OM pore complex, and it is also thought to be involved in the stability and/or gating of the OM complex (18–20). In the OM, PilQ forms a homooligomeric ring that serves as a conduit for T4P (21–23).

PilQ is a member of the secretin protein family. Proteins belonging to this family are present in many Gram-negative bacteria and are components of T4PSs, T2SSs, type III secretion systems (T3SSs), and extrusion systems of filamentous phages (24). Secretins are multidomain proteins with a signal sequence and a conserved C-terminal OM-spanning domain. Most secretins contain multiple copies of an N-terminal α/β domain (the N domains). PilQ proteins are integral OM proteins and form large gated channels. Oligomeric secretin complexes with different

Significance

Type IV pili (T4P) are ubiquitous and versatile bacterial cell surface structures involved in different processes like adhesion to host cells, biofilm formation, motility, and DNA uptake. T4P play an important role in the pathogenesis of many bacteria. We identify a protein whose presence in bacterial genomes is strongly linked to the presence of T4P systems and that is involved in the surface assembly of T4P. TsaP, the T4P secretin-associated protein is proposed to anchor the outer membrane secretin complex to the peptidoglycan and/or to align the secretin to inner membrane components.

Author contributions: K.S., S.J., C.F., M.T.W.-B., D.A.S., A.W., S.H., A.K., E.J.B., L.S.-A., and C.v.d.D. designed research; K.S., S.J., C.F., M.T.W.-B., D.A.S., I.B., A.W., S.H., J.K., and A.K. performed research; K.S., S.J., C.F., M.T.W.-B., D.A.S., I.B., A.W., S.H., J.K., A.K., E.J.B., L.S.-A., and C.v.d.D. analyzed data; and K.S., S.J., C.F., S.H., A.K., E.J.B., L.S.-A., and C.v.d.D. wrote the paper.

The authors declare no conflict of interest.

This article is a PNAS Direct Submission.

Freely available online through the PNAS open access option.

[1]K.S. and S.J. contributed equally to this work.

[2]Present address: Department of Molecular Microbiology, Groningen Biomolecular Sciences and Biotechnology Institute, University of Groningen, Nijenborgh 7, 9747 AG, Groningen, The Netherlands.

[3]To whom correspondence should be addressed. E-mail: does@mpi-marburg.mpg.de.

This article contains supporting information online at www.pnas.org/lookup/suppl/doi:10.1073/pnas.1322889111/-/DCSupplemental.

symmetries have been identified. Structural characterization by EM of purified PilQ from *Neisseria meningitidis* showed a dodecameric structure with a chamber sealed at both ends (25, 26), whereas the T2SS secretins PulD (27) and GspD (28) of the *Klebsiella oxytoca* pullanase and *Vibrio cholerae* toxin secretion systems, respectively, showed dodecameric structures with a chamber open at the periplasmic side and closed at the OM side. The structure of the InvG secretin complex of the T3SS of the *Salmonella typhimurium* needle complex showed 15-fold symmetry and is open at both ends (29), and the phage pIV secretin showed 14-fold symmetry (30). The structure of the C-terminal OM-spanning domain involved in multimer formation is currently not known. Crystal structures of the periplasmic N domains of GspD of the T2SS of enterotoxigenic *Escherichia coli* (31), of EscC of the T3SS of *S. typhimurium* (32), and of *N. meningitidis* PilQ (25) showed that these domains consist of α-helices packed against three-stranded β-sheets. Secretins of T4P systems also contain B domains, which are not present in other secretins and are located N-terminal to the N domains. The structure of the B2 domain of *N. meningitidis* PilQ consists of several β-strands (25). Remarkably, when the sequence conservation of the B2 domain was mapped to the structure of the B2 domain of *N. meningitidis* PilQ, a highly conserved patch was identified that was proposed to form the binding site for a currently unidentified T4PS protein (25).

Secretins interact with several other proteins. Pilotin proteins are small lipoproteins that interact with the extreme C terminus of secretins and are responsible for OM targeting and oligomerization of secretins (33–38). Secretins of T4PSs also interact with the alignment complex. For *N. meningitidis*, *Pseudomonas aeruginosa*, and *M. xanthus* PilQ, a direct interaction was demonstrated between the respective PilPs and the N0 domains of the PilQs (25, 39, 40). Recently, ExeA of the T2SS of *Aeromonas hydrophila* (41) and FimV of the T4PS of *P. aeruginosa* (42) were also implicated in secretin assembly. They contain, respectively, PF01471 and LysM peptidoglycan (PG)-binding domains that might attach them to the PG. However, neither of these two proteins is ubiquitously conserved in bacteria assembling T4P.

We have previously shown that the PilQ secretin of *N. gonorrhoeae* embedded in OM sheets is surrounded by a peripheral structure, which is formed by an additional peripheral ring as well as spikes (43). The proteins that make up these structures are not known. Here, we identify a widely conserved protein, which we name T4P secretin-associated protein (TsaP), that is important for the formation of the peripheral structure. Phylogenomic analysis of 450 genomes of Proteobacteria showed that the presence of the *tsaP* gene is strongly linked to the presence of genes for T4aPSs. We characterize the TsaP protein and demonstrate the importance of TsaP for T4aP assembly in the two phylogenetically widely separated model organisms *N. gonorrhoeae* and *M. xanthus*.

Results

Identification of a Protein Associated with Secretin Complexes of T4P in *N. gonorrhoeae*. Previous transmission EM studies of native PilQ complex of *N. gonorrhoeae* embedded in OM sheets showed that the PilQ secretin ring is surrounded by an additional peripheral structure that consists of a peripheral ring and seven extending spikes (43) (Fig. 1 *A* and *E*). To identify the protein(s) that form the peripheral structure, we first attempted to solubilize and purify the complex from isolated membranes. As has been done previously for *N. meningitidis* PilQ (44), a His_8-tag was introduced into the small basic repeat region of PilQ of the *N. gonorrhoeae* WT strain MS11, generating strain SJ004-MS. A screen of several detergents showed that only small amounts of His_8-PilQ could be solubilized from isolated membranes and purified by Ni^{2+}-affinity chromatography. The His_8-PilQ–containing elution fractions were analyzed by EM. Fig. S1 shows an overview of isolated particles obtained from purification using 4% (wt/vol) sulfobetaine 3-12 to solubilize and purify the complex. Single-particle alignment of these particles showed a structure consisting of a single ring (Fig. 1 *B* and *F*) with a diameter (150 Å) similar to that observed for PilQ complexes from *N. meningitidis* (44). Comparison of these particles with the previously described class average of the secretin complex embedded in OM sheets [i.e., in its native OM environment; Fig. 1 *A* and *E* (43)] showed that isolated His_8-PilQ has the same size and shape as the inner ring of this structure. However, the additional features (i.e., peripheral ring, spikes) were lost during solubilization and purification. This observation explains why these features have not been detected in previously described PilQ purifications (21, 22, 45). At the obtained resolution, individual domains of the His_8–PilQ complex are not well resolved; however, as observed previously (43), after imposing 14-fold symmetry, features become more pronounced compared with any other imposed symmetry between 12-fold and 16-fold, suggesting a 14-fold symmetry for the *N. gonorrhoeae* PilQ multimer (Fig. 1*F*). Because the peripheral ring and spikes were lost during solubilization and purification, we analyzed the nonsolubilized *N. gonorrhoeae* membrane fractions by SDS/PAGE. These fractions contained significant amounts of His_8-PilQ along with several other proteins (Fig. 2*A*). Identification of these proteins by MS identified EF-Tu, OMP I, OMP III, and a peroxiredoxin 2 family protein. These proteins were identified in a proteome study of *N. meningitidis* as four of the five most abundantly expressed proteins (46). MS also identified PilQ and the conserved hypothetical protein NGFG_01788, which were not identified as highly abundant proteins in the proteomics study mentioned (46). NGFG_01788 is a 45.5-kDa protein containing a type I signal sequence, an N-terminal LysM domain, and a C-terminal part of unknown function (Fig. 2*B*). The LysM domain is a widespread protein domain involved in PG binding. Protein BLAST (BLASTP) protein analysis and alignment identified many NGFG_01788 homologs that are conserved over the entire length of NGFG_01788 (Fig. S2) and widespread among Gram-negative bacteria. Importantly, as shown in Fig. S2, the conserved residues in other LysM domains are also conserved in the LysM domains of homologs of NGFG_01788 (47, 48).

Based on the presence of NGFG_01788 in the nonsolubilized membrane fractions together with His_8-PilQ, the presence of the LysM domain, and its co-occurrence with T4PS genes (see below), we hypothesized that NGFG_01788 is a component of the secretin

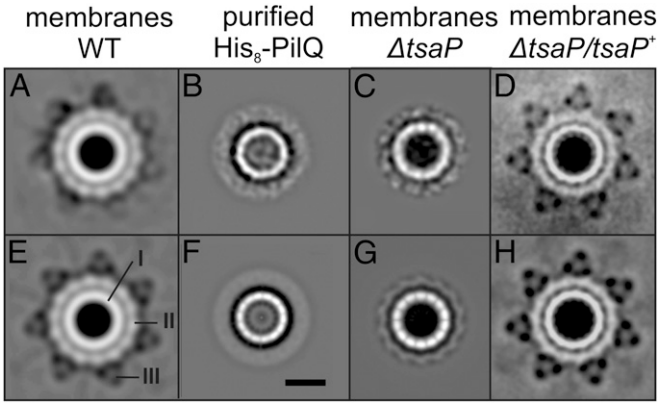

Fig. 1. Projection maps of single-particle EM analysis of the PilQ complex from *N. gonorrhoeae*. Projection maps of class averages of single-particle EM images obtained from membranes isolated from the WT (*A* and *E*), the *ΔtsaP* strain (*C* and *G*), and the *ΔtsaP/tsaP*$^+$ strain (*D* and *H*) grown in the presence of 1 mM IPTG are shown. (*B* and *F*) Class averages of single-particle EM images of the solubilized and purified His_8–PilQ complex. Projection maps without (*A*–*D*) and with (*E*–*H*) 14-fold imposed symmetry are depicted. I, II, and III indicate the inner ring, the peripheral ring, and the spikes, respectively. (Scale bar: 10 nm.)

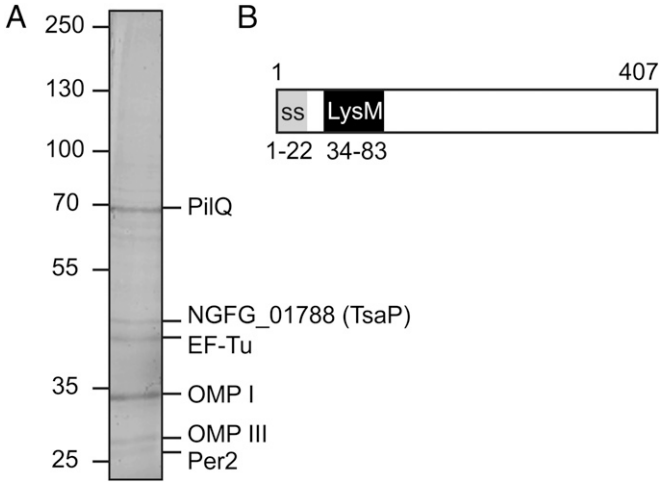

Fig. 2. Identification of TsaP (NGFG_01788). (*A*) Coomassie-stained SDS/PAGE of the nonsolubilized fraction of SB3-12–treated OMs. Analysis by MS identified PilQ, TsaP (NGFG_01788), elongation factor Tu (EF-Tu), OM protein I (OMP I), OM protein III (OMP III), and a peroxiredoxin 2 (Per2) family protein. (*B*) Domain structure of TsaP. The signal sequence (ss) and LysM domain are depicted.

complex that might anchor the complex to the PG. Henceforth, we refer to NGFG_01788 as TsaP, the T4P secretin-associated protein.

Analysis of TsaP in Membranes. To characterize the function of TsaP in *N. gonorrhoeae*, a *ΔtsaP* mutant was generated in the WT strain by insertion duplication mutagenesis (49). Moreover, a *ΔtsaP* complementation strain was generated by the ectopic insertion of a copy of *tsaP* under control of the *lac* promoter (*ΔtsaP/tsaP*$^+$) (50). Unless otherwise indicated, the *ΔtsaP/tsaP*$^+$ strain was grown in the presence of 1 mM isopropyl-β-D-thiogalactoside (IPTG). Western blotting on whole-cell extracts using α-TsaP antibodies demonstrated the presence of a protein of the expected size that was not detected in the *ΔtsaP* strain, demonstrating that the α-TsaP antibodies are specific for TsaP. Quantification showed that in whole cells, the amount of TsaP was twofold increased in the *ΔtsaP/tsaP*$^+$ complementation strain compared with WT cells (Fig. 3*A*). Immunoblotting on whole-cell extracts using the α-PilE antibodies showed that all four strains accumulated similar amounts of the PilE pilin protein. PilE of the *ΔpilQ* strain migrates slightly slower on SDS/PAGE, which is most likely caused by an altered posttranslational modification (51).

To determine directly whether TsaP is associated with membranes, total membranes were isolated from the WT, *ΔpilQ*, *ΔtsaP*, and *ΔtsaP/tsaP*$^+$ strains. PilQ forms a highly SDS-stable oligomeric complex that migrates as a high-molecular weight complex in SDS/PAGE. Coomassie staining of SDS/PAGE gels of isolated membranes showed that the high-molecular weight PilQ complex was present in membranes from the *ΔtsaP* and *ΔtsaP/tsaP*$^+$ strains at similar levels as observed in WT (Fig. 3*B*). Thus, neither the level nor the oligomerization of PilQ is affected in *ΔtsaP* and *ΔtsaP/tsaP*$^+$ strains. The PilQ oligomer can be dissociated before SDS/PAGE analysis by treatment with hot phenol. Phenol-treated membranes were analyzed after SDS/PAGE and Western blotting with antibodies raised against TsaP, PilQ, and the pilin PilE (Fig. 3*C*). These experiments demonstrated that the PilQ monomer accumulated at similar levels in the WT, *ΔtsaP*, and *ΔtsaP/tsaP*$^+$ strains. In isolated total membranes, *ΔtsaP/tsaP*$^+$ and WT showed similar levels of TsaP accumulation (Fig. 3*C*); however, the level of TsaP was reduced in the *ΔpilQ* mutant, suggesting that either membrane insertion or membrane association of TsaP depends on PilQ. As was observed for whole-cell extracts, the level of PilE was comparable in membranes isolated from the WT, *ΔpilQ*, *ΔtsaP*, and *ΔtsaP/tsaP*$^+$ strains (Fig. 3*C*), again showing that all strains expressed the pilin subunit. To test whether TsaP is more stably associated with membranes containing PilQ, total membranes isolated from the WT and *ΔpilQ* strains were incubated with 7.5 M urea. Incubation of membranes with 7.5 M urea is a common method to remove membrane-associated but not membrane-inserted proteins (52). Even after two washes, TsaP was only partially dissociated from WT membranes containing PilQ (Fig. 3*D*), suggesting that TsaP is either membrane-inserted or very tightly bound to the membrane. Remarkably, when membranes derived from the *ΔpilQ* mutant were treated with 7.5 M urea, TsaP was fully removed. Thus, tight association with or integration of TsaP in the OM depends on PilQ. We speculate that the reduced levels of TsaP observed in total

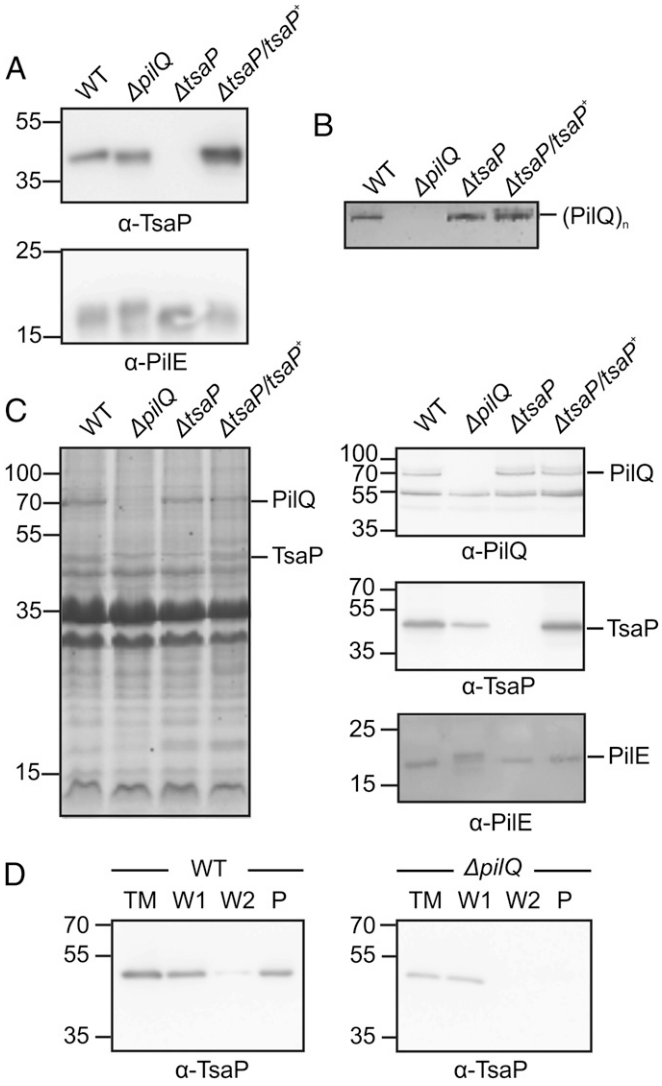

Fig. 3. Membrane binding of TsaP depends on PilQ. (*A*) Immunoblot analysis of equal amounts of total cell extracts of the WT, *ΔpilQ*, *ΔtsaP*, and *ΔtsaP/tsaP*$^+$ strains grown in the presence of 1 mM IPTG using α-TsaP and α-PilE antibodies. (*B*) Upper part of Coomassie-stained SDS/PAGE of nonphenol-treated OM fractions isolated from the indicated *N. gonorrhoeae* strains. (*C*, *Left*) Coomassie-stained SDS/PAGE of phenol-treated membrane fractions from the indicated strains. (*C*, *Right*) Immunoblot analysis of the same samples using α-TsaP, α-PilQ, and α-PilE antibodies. (*D*) Total membranes (TM) derived from *N. gonorrhoeae* WT (*Left*) and the *ΔpilQ* mutant (*Right*) were treated twice for 30 min with 7.5 M urea. After centrifugation, the supernatants (W1 and W2) and the resuspended membrane pellets (P) were analyzed by immunoblot analysis using α-TsaP antibodies.

membranes in the *ΔpilQ* strain (Fig. 3*C*) reflect the lack of tight association or integration of TsaP in the OM in the absence of PilQ or that PilQ functions to stabilize TsaP. As shown below, TsaP binds to PG. Therefore, it also remains a possibility that TsaP associates more strongly with PG in the absence of PilQ than in the presence of PilQ. If that were the case, less TsaP would be recovered in the membrane fraction in the absence of PilQ.

TsaP Binds to PG. TsaP contains an N-terminal LysM domain. To test whether TsaP is able to bind and/or hydrolyze PG, His_{10}-TsaP and murein sacculi of *N. gonorrhoeae* were purified (Fig. S3 *A* and *B*). In a sedimentation assay, TsaP was found in the supernatant in the absence of murein sacculi and was sedimented to the pellet fraction in the presence of murein sacculi (Fig. S3*C*), demonstrating that TsaP binds to isolated murein sacculi. Purified TsaP was also tested in a zymogram assay (Fig. S3*D*), but no hydrolysis of *N. gonorrhoeae* murein could be detected, whereas lysozyme and mutanolysin, as expected, both hydrolyze PG. We conclude that TsaP binds PG.

Lack of TsaP Affects Surface Assembly of T4P. On agar plates, gonococci assembling T4P on their cell surface form small, compact colonies with a sharp edge. Nonpiliated cells form flat colonies with a larger diameter and a "fuzzy" edge (53). To understand the function of TsaP further, the WT, *ΔpilQ*, *ΔtsaP*, and *ΔtsaP/tsaP*$^+$ strains were analyzed on agar plates (Fig. S4). WT and the *ΔpilQ* mutant showed colony morphologies corresponding to piliated and nonpiliated cells, respectively. The *ΔtsaP* mutant and the *ΔtsaP/tsaP*$^+$ strain grown in the absence of IPTG showed colony morphologies matching those of nonpiliated cells. Importantly, in the presence of IPTG, the *ΔtsaP/tsaP*$^+$ strain showed a colony morphology matching that of piliated cells. Thus, deletion of *tsaP* resulted in loss of the piliated colony morphology. The *ΔtsaP* and the *ΔtsaP/tsaP*$^+$ strains grown in the absence of IPTG also showed slightly decreased growth on plates, but longer incubation did not result in a piliated colony morphology.

In a next step, WT, *ΔtsaP*, and *ΔtsaP/tsaP*$^+$ cells were negatively stained for subsequent EM (Fig. 4). All strains showed OM vesicles (blebs) either as single blebs or in longer chains (54, 55). In WT and the *ΔtsaP/tsaP*$^+$ strain, single and bundled T4P were observed. In contrast, T4P in the *ΔtsaP* mutant were only observed in membrane protrusions, which were filled with up to 10 T4P. This strongly resembles the phenotype of the previously described *ΔpilQ/ΔpilT* double mutant in which T4P are assembled but cannot pass the OM, and therefore form OM protrusions. Similar to the *ΔtsaP* mutant, the *ΔpilQ/ΔpilT* mutant also showed slight growth retardation and a colony morphology matching that of nonpiliated cells (56). We conclude that in the *ΔtsaP* mutant, T4P are formed but are unable to pass the OM efficiently, and therefore assemble in OM protrusions and are not displayed on the cell surface.

Peripheral Structure of the Secretin Complex Is Lost in the *ΔtsaP* Mutant. To determine whether the deletion of *tsaP* affected the structure of the secretin complex in its native OM environment, OMs isolated from the *ΔtsaP* and *ΔtsaP/tsaP*$^+$ strains were studied by transmission EM followed by single-particle averaging (43). A comparison of the projection maps of the secretin complexes obtained from membranes of the *ΔtsaP* (Fig. 1 *C* and *G*) and *ΔtsaP/tsaP*$^+$ (Fig. 1 *D* and *H*) strains with projection maps obtained from WT membranes (Fig. 1 *A* and *E*) showed that the peripheral ring and the spikes are lost in the *ΔtsaP* mutant and that they are recovered in the *ΔtsaP/tsaP*$^+$ strain. The structures observed in membranes of the *ΔtsaP* mutant strongly resemble the structure of the isolated PilQ complex (Fig. 1*B*). The 2D map of the *ΔtsaP/tsaP*$^+$ particle was obtained at slightly higher resolution than the map of the WT particle. The structure in Fig. 1*D* is seen in a slightly tilted top-view position. A small protein domain is visible inside the inner rings, especially in the lower half. It is present in 14 copies. This becomes even clearer after imposing a high-pass filter on the image (Fig. S5). These analyses demonstrate that the *N. gonorrhoeae* PilQ secretin complex has a 14-fold symmetry.

Loss of the peripheral structure in the *ΔtsaP* mutant, combined with the observations that the membrane association/integration of TsaP depends on PilQ, suggest that PilQ and TsaP interact directly and that at least part of the peripheral structure around the PilQ secretin is formed by TsaP. We have previously reported that in *N. meningitidis*, which also encodes a TsaP homolog, the secretin structure contains the inner and peripheral rings but that the spikes are absent (43). Similarly, the spikes, but not the peripheral ring, are lost in the *N. gonorrhoeae ΔpilP and ΔpilF* mutants, whereas the spikes are still made in the *ΔpilW* and *ΔpilC* mutants (43). Immunoblotting of whole-cell extracts and of isolated membranes from the *ΔpilP*, *ΔpilF*, *ΔpilW*, and *ΔpilC* mutants demonstrated that they contained similar levels of TsaP as the WT and that TsaP associated with the OM as in WT (Fig. S6). Because loss of the peripheral ring is only observed in the *ΔtsaP* mutant and the tight association of TsaP with the OM depends on PilQ and occurs in the absence of the spikes, we suggest that TsaP forms, or is part of, the peripheral ring.

TsaP Homologs Are Specifically Found in Bacteria Encoding T4aPSs. As mentioned, TsaP homologs are widespread in Gram-negative bacteria. Based on our *N. gonorrhoeae* analyses, we hypothesized that TsaP homologs may also be important for T4P function in these bacteria. To test this hypothesis, we set out to determine whether TsaP homologs are specifically present in bacteria containing T4PSs. In Neisseriales, *tsaP* is not located in the

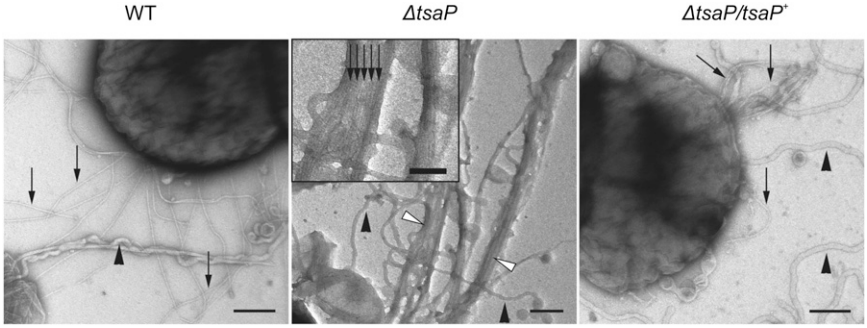

Fig. 4. Deletion of TsaP leads to formation of membrane protrusions containing T4P in *N. gonorrhoeae*. An EM analysis of WT, *ΔtsaP*, and *ΔtsaP/tsaP*$^+$ strains grown in the presence of 1 mM IPTG was performed. Cells were applied to carbon-coated copper grids, washed twice with double-distilled water, and subsequently stained with uranyl acetate before investigation via EM. T4P (black arrows) and membrane blebs (black arrowheads) are shown. (*Inset*) Membrane protrusions (white arrows) observed in the *ΔtsaP* mutant are filled with T4P. (Scale bars: main images, 200 nm; *Inset*, 50 nm.)

vicinity of genes associated with T4PSs. Synteny analysis of homologs of *tsaP* also did not reveal the presence of genes encoding proteins of T4PSs in close proximity. Similarly, genes encoding pilotins are found separated from other T4PS genes. To test whether there is a correlation between the occurrence of T4PSs in a genome and the presence of a TsaP homolog, the reciprocal BLASTP method (57) was performed with six marker proteins whose presence is indicative of T4PSs (PilQ, PilF, PilT, PilM, PilN, and PilO). When four of the six proteins were identified within a genome, this genome was considered to contain a T4P system. Divergent T4P systems in more phylogenetically distant organisms might not be identified due to the stringent thresholds needed to distinguish between T4P and T2SSs. Therefore, we focused on 450 genomes available for Proteobacteria. A list of genes encoding the T4P diagnostic proteins and TsaP homologs in the different genomes is given in Dataset S1. The distribution of the TsaP homologs and the representatives of T4PSs as identified by reciprocal BLAST analysis are shown in Fig. 5. Using reciprocal BLASTP analysis, four of the six T4PS diagnostic genes were found in 171 of the 450 genomes. In 155 of these 171 genomes, genes encoding TsaP homologs were identified. Only one TsaP homolog was detected in the remaining 279 genomes. This demonstrated a strong link between the presence of TsaP and the presence of a T4PS. Three other LysM domain-containing proteins (MltD, a membrane-bound lytic murein transglycosylase D; AmiC, the *N*-acetylmuramoyl-L-alanine amidase; and FimV, the PG-binding protein) were also included in our analysis (Dataset S1). No relation was found between the presence of MltD or AmiC and the presence of T4PSs. FimV homologs could be identified in 114 of the 171 genomes encoding a T4PS and in 23 of the 279 genomes that did not encode a T4PS, demonstrating that although not as strongly as observed for TsaP, the presence of a FimV homolog also correlated with the presence of T4PSs. Many bacteria that contain a T4PS also contain both a TsaP homolog and a FimV homolog. We were unable to find representative proteins and thresholds suitable to differentiate between T4aPSs, T4bPSs and T2SSs reliably using the reciprocal BLASTP method; therefore, we manually screened genomes that did not encode a T4aPS but encoded either a T4bPS or a T2SS for the presence of a TsaP homolog. No homologs of TsaP were identified on the R64 plasmid or in the genomes of enteropathogenic *E. coli* and *Aggregatibacter actinomycetemcomitans*, which encode a T4bPS, or in the genomes of *Klebsiella* spp. and *Yersinia enterocolitica*, which contain a T2SS but not a T4aPS (Table S1). Therefore, we conclude that a strong correlation exists between the presence of TsaP homologs and T4aPSs but that this correlation does not seem to exist for TsaP and T4bPSs or T2SSs.

TsaP Ortholog of *M. xanthus* Is Important for T4P Assembly. To determine whether the importance of TsaP in T4P formation is conserved in other bacteria, we analyzed the function of TsaP in the δ-proteobacterium *M. xanthus*. Cells of *M. xanthus* are rod-shaped and move over surfaces using two different motility systems: gliding motility and T4P-dependent motility (58). In *M. xanthus*, T4P localize to the leading cell pole (59). The *M. xanthus* TsaP homolog is encoded by MXAN_3001. *M. xanthus* genes and proteins are denoted with an MX subscript, and MXAN_3001 is named $TsaP_{MX}$. To test whether $TsaP_{MX}$ functions in T4P assembly, an in-frame deletion of $tsaP_{MX}$ ($\Delta tsaP_{MX}$) and a complementation strain in which $tsaP_{MX}$ was expressed from the constitutive *pilA* promoter ($\Delta tsaP_{MX}/tsaP_{MX}^{+}$) were generated. SDS/PAGE of whole-cell lysates followed by Western blotting using the α-$PilQ_{MX}$ antibody showed that, similar to *N. gonorrhoeae*, the assembly and stability of $PilQ_{MX}$ were not affected by the deletion of $tsaP_{MX}$ (Fig. 6*A*). As shown by Western blotting using a α-$TsaP_{MX}$ antibody, $TsaP_{MX}$ accumulated in WT and in the complementation $\Delta tsaP_{MX}/tsaP_{MX}^{+}$ strain but not in the $\Delta tsaP_{MX}$ mutant. Importantly, the level of $TsaP_{MX}$ was strongly reduced in total cell extracts of the $\Delta pilQ_{MX}$ mutant (Fig. 6*B*). In eight other mutants of T4PS proteins ($\Delta pilA_{MX}$, $\Delta pilB_{MX}$, $\Delta pilT_{MX}$, $\Delta pilC_{MX}$, $\Delta pilM_{MX}$, $\Delta pilN_{MX}$, $\Delta pilO_{MX}$, and $\Delta pilP_{MX}$), $TsaP_{MX}$ accumulated as in WT cells (Fig. S7*A*). In addition to PilQ, TsaP accumulation in total cell extracts depended on the pilotin Tgl, which is important for PilQ multimer formation (Fig. S7*A*).

To determine whether lack of $TsaP_{MX}$ affects T4P-dependent motility in *M. xanthus*, WT as well as the $\Delta pilQ_{MX}$, $\Delta tsaP_{MX}$, and $\Delta tsaP_{MX}/tsaP_{MX}^{+}$ strains were spotted on 0.5% agar plates, which is favorable to T4P motility only (Fig. 6*C*). The flares, which are typical of T4P-dependent motility, were observed for WT but not in the $\Delta pilQ$ mutant, and were strongly reduced in the $\Delta tsaP_{MX}$ mutant. The motility defect in the $\Delta tsaP_{MX}$ mutant was fully complemented by ectopic expression of $tsaP_{MX}^{+}$. Consistent with these observations, EM analyses revealed that $TsaP_{MX}$ is important for T4P formation. As observed previously (59), WT cells contained four to 10 T4P located at one pole, whereas no T4P were observed on cells of the $\Delta pilA_{MX}$ mutant, which lacks the T4P pilin subunit (Fig. 6 *D* and *E*). Importantly, in the $\Delta tsaP_{MX}$ mutant, ∼40% of cells contained one to two T4P at one pole, but most cells (>60%) did not contain T4P. We conclude that $TsaP_{MX}$ is important for T4P surface assembly, and therefore T4P-dependent motility.

$TsaP_{MX}$ Localizes in a $PilQ_{MX}$-Dependent Manner to the Cell Pole. Because T4P assemble at only one pole at a time in *M. xanthus*, *M. xanthus* is an excellent organism in which to study the localization and assembly of components of the T4PS. With the exception of the pilin subunit PilA and the pilotin Tgl, the proteins

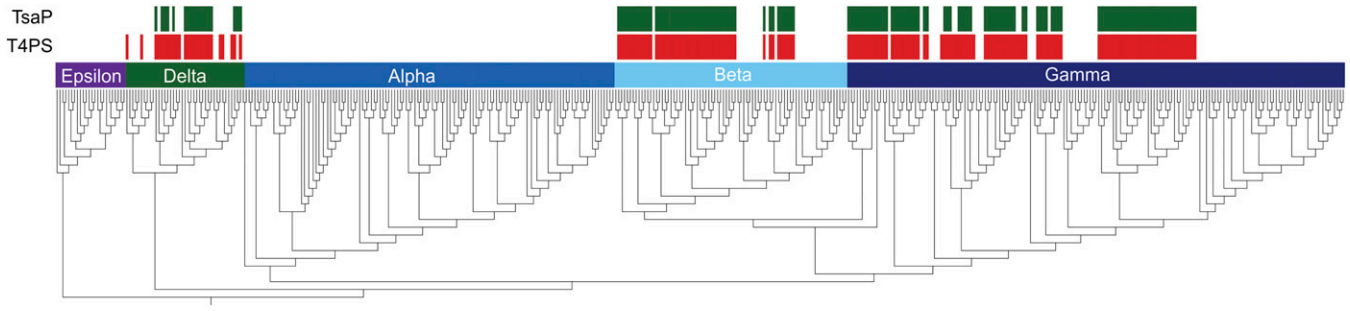

Fig. 5. Identification of genes encoding TsaP homologs and T4aPS-related genes in different genomes. A reciprocal BLAST analysis was performed for six proteins representative of T4aPSs (PilQ, PilT, PilF, PilM, PilN, and PilO), as well as for TsaP, to identify the different proteins in 450 proteobacterial genomes. Results were plotted on the 16S RNA phylogenetic tree. Colored boxes indicate the presence of a TsaP ortholog or the presence of at least four of the six proteins representative of T4aPSs.

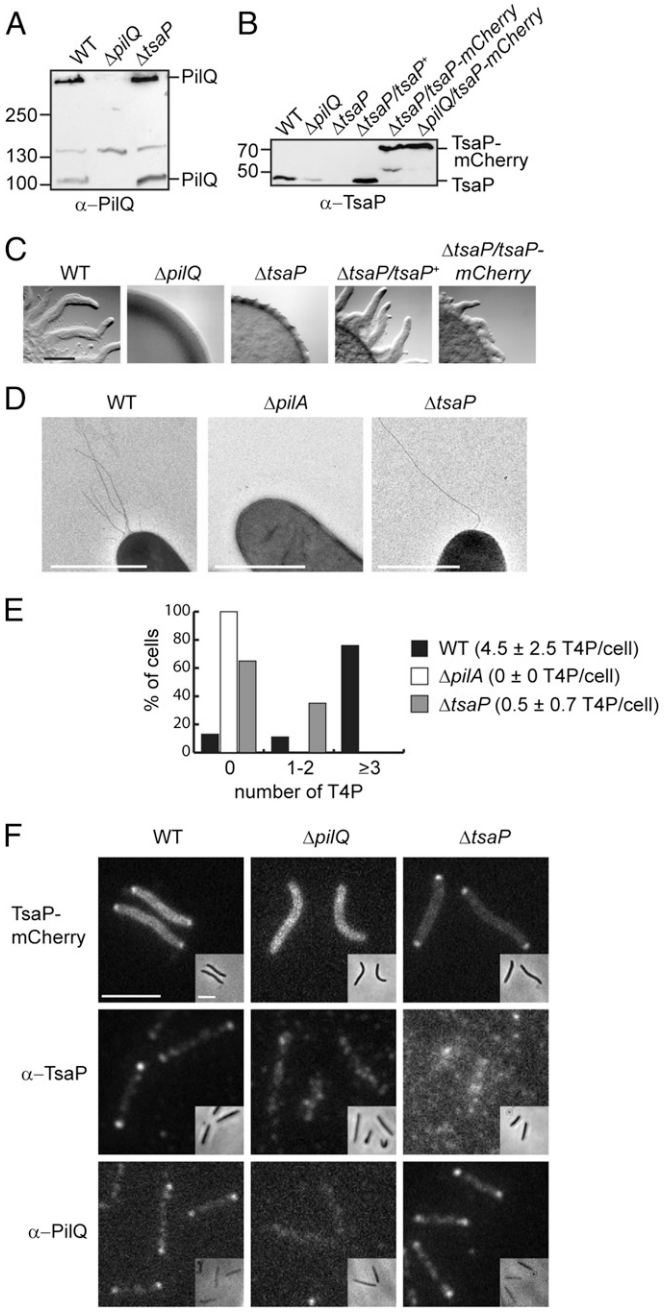

Fig. 6. Characterization of TsaP of *M. xanthus*. (*A*) $PilQ_{MX}$ accumulates independently of $TsaP_{MX}$. Equal amounts of total cell extracts of the indicated strains were separated by SDS/PAGE and analyzed by immunoblots with the α-$PilQ_{MX}$ antibody. The upper and lower bands correspond to multimeric and monomeric $PilQ_{MX}$, respectively. (*B*) $TsaP_{MX}$ accumulation depends on $PilQ_{MX}$ (as in *A* but analyzed with the α-$TsaP_{MX}$ antibody). $TsaP_{MX}$ and $TsaP_{MX}$-mCherry are indicated. (*C*) $TsaP_{MX}$ is important for T4P-dependent motility. The indicated *M. xanthus* strains were incubated at 32 °C for 24 h on 0.5% agar/0.5% CTT medium. (Scale bar: 1 mm.) (*D*) Lack of $TsaP_{MX}$ reduces the number of T4P. Cells from exponentially growing cultures were visualized by EM after staining with uranyl acetate. (Scale bars: 1 μm.) (*E*) Histogram summarizes the number of T4P per cell of the indicated strains (n = 19–55). Mean values and SDs for each strain are indicated. (*F*) $TsaP_{MX}$ localizes preferentially to the cell poles and is dependent on $PilQ_{MX}$, whereas bipolar PilQ localization is independent of $TsaP_{MX}$. (*Top*) Fluorescence microscopy and phase-contrast images (*Insets*) of WT, Δ$pilQ_{MX}$, and Δ$tsaP_{MX}$ strains expressing $TsaP_{MX}$-mCherry. (*Middle* and *Bottom*) Fluorescence microscopy and phase-contrast images of fixed cells probed with α-$TsaP_{MX}$ or α-$PilQ_{MX}$ antibodies. (Scale bar for main figure and *Inset*: 5 μm.)

of the T4PS in *M. xanthus* are polarly localized and interact to form polarly localized T4PS complexes (40, 60, 61). If $TsaP_{MX}$ interacts with $PilQ_{MX}$ to form the peripheral structure of the secretin complex, $TsaP_{MX}$ would be predicted to colocalize with $PilQ_{MX}$ and localization of $TsaP_{MX}$ and $PilQ_{MX}$ might depend on each other. To determine the localization of $TsaP_{MX}$, $TsaP_{MX}$-mCherry fusion was expressed in WT, Δ$pilQ_{MX}$, and Δ$tsaP_{MX}$ strains. $TsaP_{MX}$-mCherry accumulated to WT levels in the Δ$pilQ_{MX}$ strain (Fig. 6*B*), suggesting that $TsaP_{MX}$ is stabilized by mCherry in the absence of PilQ. In motility assays, the motility defect caused by Δ$tsaP_{MX}$ was partially complemented by $TsaP_{MX}$-mCherry (Fig. 6*C*), suggesting that the fusion protein is not fully active. Therefore, we determined the localization of TsaP using TsaP-mCherry, as well as by immunofluorescence microscopy using α-$TsaP_{MX}$ antibodies. In immunofluorescence microscopy, PilQ localized to both poles in WT as previously reported. A similar localization pattern was observed in the Δ$tsaP_{MX}$ mutant. Localization of $TsaP_{MX}$ using immunofluorescence showed that $TsaP_{MX}$ localized to both poles in WT. Similarly, TsaP-mCherry localized to both poles. Importantly, the polar localization of TsaP observed by immunofluorescence and TsaP-mCherry was lost in the Δ$pilQ_{MX}$ mutant. Moreover, analysis of the localization of TsaP-mCherry in a panel of *M. xanthus* mutants lacking individual components of the T4PS demonstrated that polar localization of TsaP-mCherry also depended on the pilotin Tgl but not on $PilA_{MX}$, $PilB_{MX}$, $PilT_{MX}$, $PilC_{MX}$, $PilM_{MX}$, $PilN_{MX}$, $PilO_{MX}$, or $PilP_{MX}$ (Fig. S7 *B–D*). Thus, localization of TsaP in *M. xanthus* specifically depends on PilQ and the Tgl pilotin but not on the other proteins involved in T4P assembly and function. Finally, in the Δ*tsaP* mutant, the localization of all polarly localized T4PS proteins was similar to that in WT (Fig. S8), demonstrating that in *M. xanthus*, the localization of none of the studied T4PS proteins depended on $TsaP_{MX}$.

We conclude that TsaP is important for efficient T4P surface assembly and T4P-dependent motility and that $TsaP_{MX}$ accumulates, localizes, and is incorporated in T4PS complexes in a strictly $PilQ_{MX}$-dependent manner. Thus, the TsaP homologs of the phylogenetically widely divergent bacteria *N. gonorrhoeae* and *M. xanthus* are both involved in correct surface assembly of T4P.

Discussion

Previous EM studies of PilQ in isolated membranes of *N. gonorrhoeae* showed that the native complex containing the PilQ secretin consists of an inner ring and an additional peripheral structure consisting of a peripheral ring with 14-fold symmetry and seven extending spikes (43). Based on structural similarity with purified PilQ of *N. meningitidis*, it was proposed that the inner ring is formed by PilQ and that the peripheral structure is formed by one or more unidentified proteins. In this study, we have identified TsaP, a 45.5-kDa protein with a signal sequence and an N-terminal LysM domain, as essential for the formation of the peripheral structure. TsaP was not found associated with solubilized and purified His_8-PilQ of *N. gonorrhoeae*; however, TsaP was, like PilQ, detected in isolated membranes and was difficult to solubilize and extract from these membranes by 7.5 M urea. Membrane integration or association of TsaP depended on the presence of PilQ, and the level of TsaP in isolated membranes was strongly reduced in a strain lacking PilQ. Comparison of the projection maps of native secretin complexes observed in OM sheets isolated from the WT and the Δ*tsaP* mutant showed that the peripheral structure was lost in the Δ*tsaP* mutant. Deletion of *tsaP* also resulted in loss of the colony morphology that corresponds to piliated cells. EM showed that T4P are still assembled in the Δ*tsaP* mutant but are not displayed on the surface of cells. Rather, the assembled T4P are found in membrane protrusions. Importantly, the peripheral ring and the spikes around PilQ and the display of T4P on the cell surface were recovered in the Δ*tsaP*/*tsaP*$^+$ complementation strain.

The presence of TsaP homologs in different genomes is strongly linked to the occurrence of T4aP systems in these genomes. No TsaP homologs were identified in species that contain only a T2SS or a T4bPS. *N. gonorrhoeae* does not contain a T2SS, but *M. xanthus* contains a T2SS of which the function is unknown. Preliminary data suggest that this T2SS is essential for growth, whereas the *M. xanthus ΔtsaP* strain did not show a growth defect, which makes it unlikely that TsaP fulfills a role in the function of T2SSs.

The strong link between the presence of TsaP and T4aPSs suggested that the TsaP homologs are also important for T4aP biogenesis in other species. This was confirmed by our studies in *M. xanthus*. In *M. xanthus*, accumulation of $TsaP_{MX}$ specifically depends on $PilQ_{MX}$ and the pilotin Tgl. Furthermore, the number of surface-assembled T4P was strongly reduced in the $\Delta tsaP_{MX}$ strain, resulting in a strong reduction of T4P-dependent motility. Protein localization studies showed that $TsaP_{MX}$ localized to the cell poles in a manner that strictly depended on $PilQ_{MX}$ and Tgl.

Overall, our data demonstrate that the presence of TsaP is strongly linked to the presence of T4PSs and that TsaP is important for the surface assembly of T4aP in both *N. gonorrhoeae* and *M. xanthus.* Several lines of evidence suggest that TsaP interacts directly with PilQ: (*i*) the peripheral ring around the inner PilQ secretin ring in OM sheets is lost in the *N. gonorrhoeae ΔtsaP* mutant (but not in the *ΔpilC*, *ΔpilW*, *ΔpilP, ΔpilE*, and *ΔpilF* mutants) and regained in the $\Delta tsaP/tsaP^{+}$ complementation strain, (*ii*) TsaP associates with the OM of *N. gonorrhoeae* in a PilQ-dependent manner (but independent of PilC, PilW, PilP, and PilF), (*iii*) TsaP is specifically stabilized by PilQ and the pilotin Tgl (but not by $PilA_{MX}$, $PilB_{MX}$, $PilT_{MX}$, $PilC_{MX}$, $PilM_{MX}$, $PilN_{MX}$, $PilO_{MX}$, or $PilP_{MX}$), and (*iv*) polar localization of $TsaP_{MX}$ in *M. xanthus* depends on $PilQ_{MX}$ and the pilotin Tgl (but not on $PilA_{MX}$, $PilB_{MX}$, $PilT_{MX}$, $PilC_{MX}$, $PilM_{MX}$, $PilN_{MX}$, $PilO_{MX}$, or $PilP_{MX}$). Thus, these data show that in *N. gonorrhoeae*, and *M. xanthus*, TsaP interacts specifically with PilQ but not with any of the other tested T4P proteins. We previously observed that in *N. meningitidis*, which also encodes a TsaP homolog, the spikes are absent (43), and the spikes were also not observed in images obtained from membranes of the *N. gonorrhoeae ΔpilP* and *ΔpilF* strains. The membranes of these strains, however, contain similar levels of TsaP as the WT. Because loss of the peripheral ring was only observed in the *ΔtsaP* mutant, we suggest that TsaP forms, or is part of, the peripheral ring. Derrick and coworkers recently solved the structures of the B2 and N0N1 domains of PilQ of *N. meningitidis* and modeled these structures on their 3D structure of full-length PilQ obtained by cryo-EM (25). They also showed that the periplasmic domain of the IM lipoprotein PilP interacts with the N0 domain and identified a highly conserved patch on the B2 domain that could form a binding site for a T4PS protein (25). The B2 domain is found in secretins of T4aPSs but not in secretins of T4bPSs or T2SSs. Because TsaP co-occurs with T4aP but not with secretins of T4bPSs or T2SSs, TsaP might bind to this conserved patch on the B2 domain. We propose that TsaP interacts directly with PilQ and is part of the peripheral structure of the secretin complex in *N. gonorrhoeae* and, based on the widespread occurrence of TsaP in genomes of organisms containing T4aPSs, that this peripheral structure is also formed in other organisms.

TsaP homologs contain a conserved N-terminal LysM domain. LysM domains bind PG and, in combination with a hydrolyzing domain (e.g., muramidase, glucosaminidase, or endopeptidase domain), can function in PG hydrolysis (47); however, the LysM domain is not thought to be enzymatically active in PG hydrolysis. Bioinformatics analyses did not identify a PG hydrolyzing domain in TsaP. Consistently, we observed that purified TsaP binds to PG but does not hydrolyze PG. This suggests that TsaP is a PG-binding protein and functions in anchoring the secretin complex to the PG via the LysM domain. Phylogenomic analyses showed that the presence of the *tsaP* gene in a genome is strongly linked to the presence of genes for T4aP systems. A main functional difference between T4aPSs and T4bPSs and T2SSs is that T4aP retracts and generates high forces (9, 10). To our knowledge, nothing is known about extension and possible retraction rates and forces for T4bPSs and T2SSs, but these rates and forces may well be much lower than observed for T4aPSs. Thus, TsaP might only be required for T4aPSs where higher rates of extension and retraction result in greater forces. Recently, FimV, a LysM domain-containing protein of *P. aeruginosa*, was also shown to be involved in T4P assembly (42, 62). FimV is a 919-aa IM protein with an N-terminal LysM domain, a transmembrane domain, and an unusually acidic C-terminal domain with tetratricopeptide repeats. Lack of FimV results in impaired T4P assembly, reduced levels of PilQ multimer formation, and lower levels of the PilMNOP proteins (42). Similar to TsaP, the presence of FimV homologs in bacterial genomes is related to the presence of a T4PS.

The *N. gonorrhoeae ΔtsaP* mutant displays membrane protrusions that are filled with multiple T4P. Similar membrane protrusions have been described for a *ΔpilQ/ΔpilT* strain of *N. gonorrhoeae* (56). These protrusions were only observed in the *ΔpilQ/ΔpilT* double mutant, but not in the *ΔpilQ* mutant (56). Koomey and coworkers (56) proposed that in the *ΔpilQ* mutant, depolymerization exceeds polymerization of pilin subunits, whereas in the *ΔpilQ/ΔpilT* double mutant, polymerization exceeds depolymerization. Because the membrane protrusions are observed in the *ΔtsaP* mutant even in the presence of PilT, pilin polymerization seems, contrary to the *ΔpilQ* mutant, not to be affected in the *ΔtsaP* mutant. Based on these comparisons, we speculate that the T4P-filled membrane protrusions formed in the absence of TsaP are either caused by (*i*) T4P that are stuck in the secretin ring and then push against the OM, resulting in the membrane protrusions, or (*ii*) misalignment of the IM/periplasmic and OM parts of the T4PS, resulting in the assembled T4P pushing against the OM. In both scenarios, the primary defect is likely caused by the lack of secretin attachment to the PG. The *M. xanthus ΔtsaP* mutant did not display T4P-filled membrane protrusions but assembled fewer T4P altogether. Although we do not know the detailed mechanism(s) underlying this difference between *N. gonorrhoeae* and *M. xanthus ΔtsaP* mutants, it is well recognized that T4PSs, although consisting of similar components overall, have minor functional differences (14). We also note that the OMs of *N. gonorrhoeae* and *M. xanthus* likely have different properties due to the presence of lipooligosaccharides in *N. gonorrhoeae* (63) vs. the presence of lipopolysaccharides in *M. xanthus* (64). Alternatively, the difference might be caused by differences between T4PS proteins in these two organisms (e.g., $PilQ_{MX}$ contains an amidase N-terminal (AMIN) domain that is not present in PilQ of *N. gonorrhoeae*). AMIN domains were recently shown to bind PG (65). All together, we conclude that TsaP in *N. gonorrhoeae*, as well as in *M. xanthus*, is important for the formation of surface-exposed T4P.

We have previously shown that the PilQ secretin of *N. gonorrhoeae* interacts with other proteins in the OM to form a large multidomain complex. Here, we identified TsaP as a likely member of this complex and show that the occurrence of TsaP in bacterial genomes is strongly linked to the presence of T4aPSs. TsaP plays an important role in pilus biogenesis in both the β-proteobacterium *N. gonorrhoeae* and the δ-proteobacterium *M. xanthus.* TsaP most likely functions in anchoring the secretin to the PG to enable the secretin to withstand the forces during pilus extension and retraction. TsaP might also function in aligning the IM and OM components of the T4PS. T4P play an important role in the pathogenesis of many bacteria. Because TsaP is found in all bacteria that express T4aP and plays an important role in T4aP biogenesis, it might be an important future drug target.

Materials and Methods

Bacterial Strains, Plasmids, and DNA Manipulations. Generation and growth of *N. gonorrhoeae* and *M. xanthus* strains are described in *SI Materials and Methods*.

Antibodies. Antibodies against *N. gonorrhoeae* PilQ and TsaP were created by Genscript against the "NKPGQYNTEVRGNKC" and "CPGRDLDNMPDQGRA" peptides, respectively. The antibodies against PilE (66) and $PilQ_{MX}$ (60) have been described previously. The antibody against $TsaP_{MX}$ was generated by Eurogentec against His_6-Δ7$TsaP_{MX}$ isolated from inclusion bodies from the *E. coli* Rosetta 2 strain containing plasmid pIMB5 using denaturing Ni^{2+}-nitrilotriacetic acid (NTA) affinity purification (a detailed protocol is provided in *SI Materials and Methods*).

Preparation of *N. gonorrhoeae* Membranes. *N. gonorrhoeae* membranes were prepared as described previously (43). To generate monomeric PilQ, samples were phenol-treated and heated as described (43, 67).

Solubilization and Purification of PilQ. To purify His_8-PilQ, membranes of *N. gonorrhoeae* SJ004-MS were solubilized for 2 h in buffer A [250 mM NaCl, 50 mM Tris (pH 7.4)] containing different detergents [1% n-dodecyl β-D-maltoside (DDM), 2% (wt/vol) 3-[(3-Cholamidopropyl)dimethylammonio]-1-propanesulfonate (CHAPS), 1% Triton X-100, 4% (wt/vol) sulfobetaine (SB) 3-10, 4% (wt/vol) SB3-12, 5% (wt/vol) SB3-14] at 4 °C. After centrifugation at 100,000 × *g* for 30 min, the supernatant was loaded onto a HIS-Select nickel affinity column (Sigma–Aldrich). After washing steps with detergent-containing buffer A and 20 or 60 mM imidazole, PilQ was eluted with detergent containing buffer A and 250 mM imidazole.

EM. To analyze purified PilQ, elution fractions of the purification were applied on carbon-coated copper grids and negatively stained with 2% (wt/vol) uranyl acetate by the droplet method as described previously (43). EM and single-particle analysis of secretin complexes from purified PilQ fractions or in isolated membranes were performed as described (43). For *N. gonorrhoeae*, transmission EM of whole cells and T4P was essentially done as described (68). For *M. xanthus*, 5-μL aliquots of exponentially growing cultures were applied to carbon-coated grids (400-square mesh). After washing two times on a drop of double-distilled water, the samples were negatively stained with 2% (wt/vol) uranyl acetate and air-dried. Transmission EM was performed on a JEOL JEM-2100 transmission electron microscope at an acceleration voltage of 120 kV, and images captured with a 2k × 2k fast scan CCD camera F214 (TVIPS).

MS of Nonsolubilized Fractions. Membranes were solubilized for 2 h in buffer A plus different detergents [1% DDM, 2% (wt/vol) CHAPS, 1% Triton, 4% (wt/vol) SB3-10, 4% (wt/vol) SB3-12, 5% (wt/vol) SB3-14] at 4 °C. After centrifugation at 100,000 × *g* for 30 min at 4 °C, the supernatant was removed and the pellet was resuspended in 250 mM NaCl and 50 mM Tris (pH 7.4). After dissociation of the multimeric PilQ complex, samples were loaded for SDS/PAGE. MS to identify the proteins excised from SDS/PAGE gels was performed as described (69).

Western Blots. Western blot analysis was performed using standard procedures. For *N. gonorrhoeae*, proteins were transferred to PVDF membranes. The α-PilQ, α-TsaP, and α-PilE antibodies were detected using alkaline phosphatase-conjugated secondary antibodies [for α-PilQ and α-TsaP, anti-rabbit antibodies (BioRad); for α-PilE, anti-mouse antibody (Sigma–Aldrich)] and CDP-Star substrate (Roche Diagnostics). For *M. xanthus*, proteins were transferred to nitrocellulose membranes. α-$TsaP_{MX}$, as well as antibodies directed toward other T4PS proteins (15, 40, 60), was detected using secondary anti-rabbit IgG peroxidase conjugate (Sigma–Aldrich) and Luminata Western HRP Substrate (Merck Millipore). Blots were developed using a LAS-4000 imager (GE Healthcare).

OM Detachment Assay. OMs were incubated in 7.5 M urea for 30 min at 4 °C on a rotary shaker. Following membrane treatment, samples were centrifuged for 30 min at 100,000 × *g* at 4 °C. Proteins in the soluble fractions were collected. The insoluble proteins were treated once more with 7.5 M urea and collected by centrifugation. Supernatant and pellet fractions were then analyzed by SDS/PAGE and immunoblotting using the α-TsaP antibodies. Before loading, soluble fractions were precipitated with trichloroacetic acid.

Purification of TsaP. His_{10}-TsaP was overexpressed in *E. coli* BL21 star (DE3) transformed with pAW001 and purified using Ni^{2+}-NTA affinity purification and size exclusion chromatography (a detailed protocol is provided in *SI Materials and Methods*).

Reciprocal BLASTP Analysis. Reciprocal BLASTP analysis was performed as described previously (57). BLASTP analyses were done with an initial expect value cutoff of 0.1 on 450 selected genomes of Proteobacteria. The PilQ (NP_253727.1), PilT (NP_249086.1; Met1-Ser119), PilF (NP_253216.1; Met1-Gly199), PilM (NP_253731.1), PilN (NP_253730.1), PilO (NP_253729.1), TsaP (NP_248710.1; Arg90-Pro341), MltD (PA1812), AmiC (PA4947), and FimV (PA3115) proteins of *P. aeruginosa* PAO1 were used as the initial query sequences in the analyses. The initial BLAST data were filtered with a query-specific expect value cutoff (PilQ, E-65; PilT, E-20; PilF, E-5; PilM, E-15; PilN, E-5, PilO, E-5; TsaP, E-3; MltD, E-5; AmiC, E-5; FimV, E-5) to eliminate nonspecific results.

***M. xanthus* Motility Assays.** Cells from exponentially growing cultures were harvested and resuspended in 1% CTT to a density of 7×10^9 cells per milliliter. Five milliliters was spotted on 0.5% agar supplemented with 0.5% CTT and incubated at 32 °C for 24 h. Colony edges were documented using a Leica MZ8 stereomicroscope and a Leica DFC280 camera.

Fluorescence Microscopy. Phase-contrast and fluorescence microscopy were done as described (70). Briefly, cells from exponentially growing cultures were transferred to a thin 1.5% (wt/vol) agar pad containing 10 mM $CaCl_2$, 10 mM $MgCl_2$, 50 mM NaCl, and 10 mM MOPS (pH 7.2) on a glass slide and covered with a coverslip. Cells were immediately visualized with a Leica DM6000B microscope using a Leica Plan Apo phase-contrast oil objective with a magnification of 100× and N.A. of 1.40 and were imaged with a Roper Photometrics Cascade II 1024 camera. Images were recorded and processed with Metamorph (Molecular Devices). Immunofluorescence was done as previously described (40). For all fluorescence microscopy, a Leica Y3 filter (excitation range of 530–560 nm, emission range of 570–650 nm) was used.

ACKNOWLEDGMENTS. This work was supported by the German Research Council within the framework of the Collaborative Research Center 987 "Microbial Diversity in Environmental Signal Response" by the Max Planck Society, by the Landes-Offensive zur Entwicklung Wissenschaftlich-ökonomischer Exzellenz Research Centre for Synthetic Microbiology, and by a fellowship from the International Max Planck Research School for Environmental, Cellular, and Molecular Microbiology (to C.F.).

1. Giltner CL, Nguyen Y, Burrows LL (2012) Type IV pilin proteins: Versatile molecular modules. *Microbiol Mol Biol Rev* 76(4):740–772.
2. Jarrell KF, Albers SV (2012) The archaellum: An old motility structure with a new name. *Trends Microbiol* 20(7):307–312.
3. Korotkov KV, Sandkvist M, Hol WG (2012) The type II secretion system: Biogenesis, molecular architecture and mechanism. *Nat Rev Microbiol* 10(5):336–351.
4. Chen I, Dubnau D (2003) DNA transport during transformation. *Front Biosci* 8:s544–s556.
5. Pelicic V (2008) Type IV pili: E pluribus unum? *Mol Microbiol* 68(4):827–837.
6. Burrows LL (2012) *Pseudomonas aeruginosa* twitching motility: Type IV pili in action. *Annu Rev Microbiol* 66:493–520.
7. Merz AJ, So M, Sheetz MP (2000) Pilus retraction powers bacterial twitching motility. *Nature* 407(6800):98–102.
8. Skerker JM, Berg HC (2001) Direct observation of extension and retraction of type IV pili. *Proc Natl Acad Sci USA* 98(12):6901–6904.
9. Clausen M, Jakovljevic V, Søgaard-Andersen L, Maier B (2009) High-force generation is a conserved property of type IV pilus systems. *J Bacteriol* 191(14): 4633–4638.
10. Maier B, et al. (2002) Single pilus motor forces exceed 100 pN. *Proc Natl Acad Sci USA* 99(25):16012–16017.
11. Freitag NE, Seifert HS, Koomey M (1995) Characterization of the *pilF-pilD* pilus-assembly locus of *Neisseria gonorrhoeae*. *Mol Microbiol* 16(3):575–586.
12. Strom MS, Nunn DN, Lory S (1993) A single bifunctional enzyme, PilD, catalyzes cleavage and N-methylation of proteins belonging to the type IV pilin family. *Proc Natl Acad Sci USA* 90(6):2404–2408.
13. Craig L, Pique ME, Tainer JA (2004) Type IV pilus structure and bacterial pathogenicity. *Nat Rev Microbiol* 2(5):363–378.
14. Takhar HK, Kemp K, Kim M, Howell PL, Burrows LL (2013) The platform protein is essential for type IV pilus biogenesis. *J Biol Chem* 288(14):9721–9728.
15. Jakovljevic V, Leonardy S, Hoppert M, Søgaard-Andersen L (2008) PilB and PilT are ATPases acting antagonistically in type IV pilus function in *Myxococcus xanthus*. *J Bacteriol* 190(7):2411–2421.
16. Satyshur KA, et al. (2007) Crystal structures of the pilus retraction motor PilT suggest large domain movements and subunit cooperation drive motility. *Structure* 15(3): 363–376.

17. Kurre R, Höne A, Clausen M, Meel C, Maier B (2012) PilT2 enhances the speed of gonococcal type IV pilus retraction and of twitching motility. *Mol Microbiol* 86(4): 857–865.
18. Tammam S, et al. (2011) Characterization of the PilN, PilO and PilP type IVa pilus subcomplex. *Mol Microbiol* 82(6):1496–1514.
19. Georgiadou M, Castagnini M, Karimova G, Ladant D, Pelicic V (2012) Large-scale study of the interactions between proteins involved in type IV pilus biology in *Neisseria meningitidis*: Characterization of a subcomplex involved in pilus assembly. *Mol Microbiol* 84(5):857–873.
20. Ayers M, et al. (2009) PilM/N/O/P proteins form an inner membrane complex that affects the stability of the *Pseudomonas aeruginosa* type IV pilus secretin. *J Mol Biol* 394(1):128–142.
21. Collins RF, Davidsen L, Derrick JP, Ford RC, Tønjum T (2001) Analysis of the PilQ secretin from *Neisseria meningitidis* by transmission electron microscopy reveals a dodecameric quaternary structure. *J Bacteriol* 183(13):3825–3832.
22. Collins RF, et al. (2004) Structure of the Neisseria meningitidis outer membrane PilQ secretin complex at 12 A resolution. *J Biol Chem* 279(38):39750–39756.
23. Genin S, Boucher CA (1994) A superfamily of proteins involved in different secretion pathways in gram-negative bacteria: Modular structure and specificity of the N-terminal domain. *Mol Gen Genet* 243(1):112–118.
24. Korotkov KV, Gonen T, Hol WG (2011) Secretins: Dynamic channels for protein transport across membranes. *Trends Biochem Sci* 36(8):433–443.
25. Berry JL, et al. (2012) Structure and assembly of a trans-periplasmic channel for type IV pili in *Neisseria meningitidis*. *PLoS Pathog* 8(9):e1002923.
26. Karuppiah V, Collins RF, Thistlethwaite A, Gao Y, Derrick JP (2013) Structure and assembly of an inner membrane platform for initiation of type IV pilus biogenesis. *Proc Natl Acad Sci USA* 110(48):E4638–E4647.
27. Chami M, et al. (2005) Structural insights into the secretin PulD and its trypsin-resistant core. *J Biol Chem* 280(45):37732–37741.
28. Reichow SL, Korotkov KV, Hol WG, Gonen T (2010) Structure of the cholera toxin secretion channel in its closed state. *Nat Struct Mol Biol* 17(10):1226–1232.
29. Schraidt O, Marlovits TC (2011) Three-dimensional model of Salmonella's needle complex at subnanometer resolution. *Science* 331(6021):1192–1195.
30. Opalka N, et al. (2003) Structure of the filamentous phage pIV multimer by cryo-electron microscopy. *J Mol Biol* 325(3):461–470.
31. Korotkov KV, Pardon E, Steyaert J, Hol WG (2009) Crystal structure of the N-terminal domain of the secretin GspD from ETEC determined with the assistance of a nanobody. *Structure* 17(2):255–265.
32. Spreter T, et al. (2009) A conserved structural motif mediates formation of the periplasmic rings in the type III secretion system. *Nat Struct Mol Biol* 16(5):468–476.
33. Gu S, Rehman S, Wang X, Shevchik VE, Pickersgill RW (2012) Structural and functional insights into the pilotin-secretin complex of the type II secretion system. *PLoS Pathog* 8(2):e1002531.
34. Tosi T, et al. (2011) Pilotin-secretin recognition in the type II secretion system of *Klebsiella oxytoca*. *Mol Microbiol* 82(6):1422–1432.
35. Korotkov KV, Hol WG (2013) Crystal structure of the pilotin from the enterohemorrhagic *Escherichia coli* type II secretion system. *J Struct Biol* 182(2):186–191.
36. Koo J, et al. (2008) PilF is an outer membrane lipoprotein required for multimerization and localization of the *Pseudomonas aeruginosa* Type IV pilus secretin. *J Bacteriol* 190(21):6961–6969.
37. Carbonnelle E, Helaine S, Nassif X, Pelicic V (2006) A systematic genetic analysis in *Neisseria meningitidis* defines the Pil proteins required for assembly, functionality, stabilization and export of type IV pili. *Mol Microbiol* 61(6):1510–1522.
38. Okon M, et al. (2008) Structural characterization of the type-III pilot-secretin complex from *Shigella flexneri*. *Structure* 16(10):1544–1554.
39. Tammam S, et al. (2013) PilMNOPQ from the Pseudomonas aeruginosa type IV pilus system form a transenvelope protein interaction network that interacts with PilA. *J Bacteriol* 195(10):2126–2135.
40. Friedrich C, Bulyha I, Søgaard-Andersen L (2014) Outside-In Assembly Pathway of the Type IV Pilus System in Myxococcus xanthus. *J Bacteriol* 196(2):378–390.
41. Li G, Miller A, Bull H, Howard SP (2011) Assembly of the type II secretion system: Identification of ExeA residues critical for peptidoglycan binding and secretin multimerization. *J Bacteriol* 193(1):197–204.
42. Wehbi H, et al. (2011) The peptidoglycan-binding protein FimV promotes assembly of the *Pseudomonas aeruginosa* type IV pilus secretin. *J Bacteriol* 193(2):540–550.
43. Jain S, et al. (2011) Structural characterization of outer membrane components of the type IV pili system in pathogenic Neisseria. *PLoS ONE* 6(1):e16624.
44. Frye SA, et al. (2006) Topology of the outer-membrane secretin PilQ from *Neisseria meningitidis*. *Microbiology* 152(Pt 12):3751–3764.
45. Balasingham SV, et al. (2007) Interactions between the lipoprotein PilP and the secretin PilQ in *Neisseria meningitidis*. *J Bacteriol* 189(15):5716–5727.
46. Hu Y, et al. (2010) Proteome analysis of *Neisseria meningitidis* serogroup strains C associated with outbreaks in China. *Biomed Environ Sci* 23(4):251–258.
47. Buist G, Steen A, Kok J, Kuipers OP (2008) LysM, a widely distributed protein motif for binding to (peptido)glycans. *Mol Microbiol* 68(4):838–847.
48. Bateman A, Bycroft M (2000) The structure of a LysM domain from *E. coli* membrane-bound lytic murein transglycosylase D (MltD). *J Mol Biol* 299(4):1113–1119.
49. Hamilton HL, Schwartz KJ, Dillard JP (2001) Insertion-duplication mutagenesis of neisseria: Use in characterization of DNA transfer genes in the gonococcal genetic island. *J Bacteriol* 183(16):4718–4726.
50. Hamilton HL, Domínguez NM, Schwartz KJ, Hackett KT, Dillard JP (2005) *Neisseria gonorrhoeae* secretes chromosomal DNA via a novel type IV secretion system. *Mol Microbiol* 55(6):1704–1721.
51. Hegge FT, et al. (2004) Unique modifications with phosphocholine and phosphoethanolamine define alternate antigenic forms of *Neisseria gonorrhoeae* type IV pili. *Proc Natl Acad Sci USA* 101(29):10798–10803.
52. van der Does C, et al. (1996) SecA is an intrinsic subunit of the *Escherichia coli* preprotein translocase and exposes its carboxyl terminus to the periplasm. *Mol Microbiol* 22(4):619–629.
53. Dillard JP (2011) Genetic manipulation of Neisseria gonorrhoeae. *Curr Protoc Microbiol* Chapter 4:Unit4A2. (Wiley, Hoboken, NJ), pp 1–24.
54. de Souza AL, Seguro AC (2008) Two centuries of meningococcal infection: From Vieusseux to the cellular and molecular basis of disease. *J Med Microbiol* 57(Pt 11): 1313–1321.
55. Remis JP, et al. (2014) Bacterial social networks: Structure and composition of *Myxococcus xanthus* outer membrane vesicle chains. *Environ Microbiol* 16(2):598–610.
56. Wolfgang M, van Putten JP, Hayes SF, Dorward D, Koomey M (2000) Components and dynamics of fiber formation define a ubiquitous biogenesis pathway for bacterial pili. *EMBO J* 19(23):6408–6418.
57. Huntley S, et al. (2011) Comparative genomic analysis of fruiting body formation in Myxococcales. *Mol Biol Evol* 28(2):1083–1097.
58. Zhang Y, Ducret A, Shaevitz J, Mignot T (2012) From individual cell motility to collective behaviors: Insights from a prokaryote, *Myxococcus xanthus*. *FEMS Microbiol Rev* 36(1):149–164.
59. Kaiser D (1979) Social gliding is correlated with the presence of pili in *Myxococcus xanthus*. *Proc Natl Acad Sci USA* 76(11):5952–5956.
60. Bulyha I, et al. (2009) Regulation of the type IV pili molecular machine by dynamic localization of two motor proteins. *Mol Microbiol* 74(3):691–706.
61. Nudleman E, Wall D, Kaiser D (2006) Polar assembly of the type IV pilus secretin in *Myxococcus xanthus*. *Mol Microbiol* 60(1):16–29.
62. Semmler AB, Whitchurch CB, Leech AJ, Mattick JS (2000) Identification of a novel gene, fimV, involved in twitching motility in *Pseudomonas aeruginosa*. *Microbiology* 146(Pt 6):1321–1332.
63. Schneider H, Griffiss JM, Williams GD, Pier GB (1982) Immunological basis of serum resistance of *Neisseria gonorrhoeae*. *J Gen Microbiol* 128(1):13–22.
64. Bowden MG, Kaplan HB (1998) The *Myxococcus xanthus* lipopolysaccharide O-antigen is required for social motility and multicellular development. *Mol Microbiol* 30(2): 275–284.
65. Rocaboy M, et al. (2013) The crystal structure of the cell division amidase AmiC reveals the fold of the AMIN domain, a new peptidoglycan binding domain. *Mol Microbiol* 90(2):267–277.
66. Nicolson IJ, Perry AC, Heckels JE, Saunders JR (1987) Genetic analysis of variant pilin genes from *Neisseria gonorrhoeae* P9 cloned in *Escherichia coli*: Physical and immunological properties of encoded pilins. *J Gen Microbiol* 133(3):553–561.
67. Hancock RE, Nikaido H (1978) Outer membranes of gram-negative bacteria. XIX. Isolation from *Pseudomonas aeruginosa* PAO1 and use in reconstitution and definition of the permeability barrier. *J Bacteriol* 136(1):381–390.
68. Bubendorfer S, et al. (2012) Specificity of motor components in the dual flagellar system of *Shewanella putrefaciens* CN-32. *Mol Microbiol* 83(2):335–350.
69. Kahnt J, et al. (2010) Profiling the outer membrane proteome during growth and development of the social bacterium *Myxococcus xanthus* by selective biotinylation and analyses of outer membrane vesicles. *J Proteome Res* 9(10):5197–5208.
70. Leonardy S, Freymark G, Hebener S, Ellehauge E, Søgaard-Andersen L (2007) Coupling of protein localization and cell movements by a dynamically localized response regulator in *Myxococcus xanthus*. *EMBO J* 26(21):4433–4444.